
DP-FEDSOFIM: DIFFERENTIALLY PRIVATE FEDERATED STOCHASTIC OPTIMIZATION USING REGULARIZED FISHER INFORMATION MATRIX

A PREPRINT

Sidhant R. Nair

Department of Mechanical Engineering
Indian Institute of Technology Delhi
New Delhi, India
me1221991@iitd.ac.in

Tanmay Sen

SQC & OR Unit
Indian Statistical Institute Kolkata
Kolkata, India
tanmay.sen@isical.ac.in

Mrinmay Sen

Department of Artificial Intelligence
Indian Institute of Technology Hyderabad
Hyderabad, India
senmrinmay@alumni.iith.ac.in

January 15, 2026

ABSTRACT

Differentially private federated learning (DP-FL) suffers from slow convergence under tight privacy budgets due to the overwhelming noise introduced to preserve privacy. While adaptive optimizers can accelerate convergence, existing second-order methods such as DP-FedNew require $O(d^2)$ memory at each client to maintain local feature covariance matrices, making them impractical for high-dimensional models. We propose DP-FedSOFIM, a server-side second-order optimization framework that leverages the Fisher Information Matrix (FIM) as a natural gradient preconditioner while requiring only $O(d)$ memory per client. By employing the Sherman-Morrison formula for efficient matrix inversion, DP-FedSOFIM achieves $O(d)$ computational complexity per round while maintaining the convergence benefits of second-order methods. Our analysis proves that the server-side preconditioning preserves (ϵ, δ) -differential privacy through the post-processing theorem. Empirical evaluation on CIFAR-10 demonstrates that DP-FedSOFIM achieves superior test accuracy compared to first-order baselines across multiple privacy regimes.

1 Introduction

Federated learning (FL) enables collaborative model training across decentralized data silos without direct data sharing, making it particularly attractive for privacy-sensitive applications such as healthcare and finance [17, 12]. However, the mere avoidance of centralized data aggregation does not guarantee formal privacy protection. Differential privacy (DP) provides a rigorous mathematical framework to bound information leakage during training [7, 8, 1], but integrating DP into federated learning introduces fundamental challenges.

The primary obstacle in differentially private federated learning is the convergence-privacy tradeoff. To achieve (ϵ, δ) -DP, gradient updates must be clipped and perturbed with Gaussian noise calibrated to the sensitivity of the mechanism [1]. In federated settings with limited communication rounds, this noise dominates the true gradient signal, leading to prohibitively slow convergence, especially under stringent privacy budgets ($\epsilon < 2$) [3].

Adaptive optimization methods have proven effective in accelerating convergence in non-private settings by exploiting curvature information [6, 13]. Recent work has extended these techniques to the DP-FL regime. DP-FedNew [14]

introduced a second-order preconditioner based on local feature covariance matrices, achieving significant speedups. However, this approach incurs $O(d^2)$ memory overhead per client and requires maintaining per-client feature statistics, which becomes prohibitive for high-dimensional models and resource-constrained edge devices.

We introduce DP-FedSOFIM (Differentially Private Second-Order Federated Information Matrix), a framework that shifts the computational burden of second-order optimization entirely to the server while preserving the convergence benefits of natural gradient descent. Our key contributions are:

- **Server-Side Second-Order Preconditioning:** We formulate a natural gradient preconditioner using the Fisher Information Matrix (FIM) constructed from noisy aggregated gradients, eliminating the need for clients to maintain $O(d^2)$ memory.
- **Efficient $O(d)$ Implementation:** By leveraging the Sherman-Morrison formula for low-rank matrix updates, we achieve $O(d)$ computational complexity per round, making our approach scalable to high-dimensional models.
- **Privacy Preservation via Post-Processing:** We prove that server-side preconditioning preserves (ϵ, δ) -DP guarantees through the post-processing theorem, as the FIM is computed on already-privatized gradient aggregates.
- **Empirical Validation:** Experiments on CIFAR-10 with ResNet-20 frozen features demonstrate that DP-FedSOFIM consistently outperforms DP-FedGD across all privacy budgets. We observe absolute accuracy improvements of up to +3.12% in the non-private baseline and +2.37% at $\epsilon = 10$. Notably, the algorithm maintains superiority even in the high-noise regime ($\epsilon \leq 1$), achieving gains of +0.42% to +0.60% under these stringent privacy constraints.

The remainder of this paper is organized as follows. Section 2 reviews related work on differentially private federated learning and second-order optimization. Section 3 presents the DP-FedSOFIM algorithm and its efficient implementation. Section 4 provides theoretical convergence guarantees and privacy analysis. Section 5 presents experimental results (to be completed with detailed results), and Section 6 concludes with discussion and future directions.

2 Related Work

2.1 Differentially Private Federated Learning

Differential privacy in federated learning has been studied extensively. The seminal work by [1] introduced the moments accountant for tracking privacy loss in iterative algorithms. [18] proposed DP-FedAvg, which applies user-level differential privacy by clipping and adding noise to client updates. Subsequent work has focused on improving the privacy-utility tradeoff through advanced privacy accounting methods [19, 5] and amplification by sampling [4]. [3] demonstrated that adaptive clipping strategies can significantly improve convergence in the DP-FL setting. More recently, [14] introduced DP-FedNew, a second-order method based on local feature covariance matrices that achieves substantial speedups over first-order baselines. However, DP-FedNew’s requirement for local $O(d^2)$ memory per client limits its applicability to high-dimensional models and resource-constrained edge devices. Our work addresses this limitation by moving second-order computation entirely to the server while maintaining $O(d)$ client-side complexity.

2.2 Adaptive and Second-Order Optimizers in Federated Learning

Adaptive optimization methods such as Adam [13] and AdaGrad [6] have become standard in centralized deep learning. Extending these methods to federated settings is non-trivial due to the need to aggregate adaptive statistics across clients [21]. FedAdam and FedYogi [21] maintain server-side adaptive learning rates but do not explicitly leverage second-order curvature information.

Natural gradient descent [2] uses the Fisher Information Matrix as a preconditioner, providing a principled approach to incorporating curvature. However, computing the exact FIM requires $O(d^2)$ storage and $O(d^3)$ inversion, making it impractical for large-scale models. Approximation methods such as K-FAC [16] and diagonal Fisher [20] reduce computational costs but introduce additional approximation errors.

DP-FedNew [14] computes local feature covariance matrices at each client, which approximates the FIM for generalized linear models. While effective, this approach requires each client to store and communicate $O(d^2)$ parameters. In contrast, DP-FedSOFIM constructs a global FIM proxy on the server using aggregated noisy gradients, achieving $O(d)$ memory complexity while preserving the benefits of second-order preconditioning.

2.3 Efficient Matrix Inversion Techniques

The Sherman-Morrison formula [23] provides an efficient method for updating matrix inverses when a matrix is modified by a rank-one perturbation. This technique has been applied in online learning [11] and recursive least squares [10]. We leverage this formula to maintain an efficient inverse of the regularized Fisher Information Matrix, enabling $O(d)$ updates per round.

3 Methodology

3.1 Problem Setup and Notation

Consider a federated learning setting with K clients, where each client $k \in [K]$ holds a private dataset \mathcal{D}_k . The goal is to minimize the empirical risk:

$$\min_{\theta \in \mathbb{R}^d} F(\theta) = \frac{1}{K} \sum_{k=1}^K F_k(\theta) \quad (1)$$

$$F_k(\theta) = \frac{1}{|\mathcal{D}_k|} \sum_{(x,y) \in \mathcal{D}_k} \ell(\theta; x, y) \quad (2)$$

where $\ell(\theta; x, y)$ is the loss function and $\theta \in \mathbb{R}^d$ represents the model parameters.

We operate under the record-level differential privacy model [1], where each training example (x, y) is considered a private record. The privacy guarantee ensures that the participation or non-participation of any single record has a bounded effect on the algorithm's output distribution.

Definition 3.1 $((\epsilon, \delta)$ -Differential Privacy). A randomized mechanism $\mathcal{M} : \mathcal{D} \rightarrow \mathcal{R}$ satisfies (ϵ, δ) -differential privacy if for all neighboring datasets $\mathcal{D}, \mathcal{D}'$ differing in at most one record and for all measurable sets $S \subseteq \mathcal{R}$:

$$\mathbb{P}[\mathcal{M}(\mathcal{D}) \in S] \leq e^\epsilon \mathbb{P}[\mathcal{M}(\mathcal{D}') \in S] + \delta \quad (3)$$

3.2 Baseline: DP-FedGD with Gradient Clipping and Noise Addition

The baseline differentially private federated gradient descent (DP-FedGD) implements record-level differential privacy via per-example gradient clipping. We operate under full client participation, where all n clients participate in every round (i.e., $K = n$).

At round t , each client i with local dataset \mathcal{D}_i of size $|\mathcal{D}_i|$ performs the following:

Per-Example Clipping: For each record $(x, y) \in \mathcal{D}_i$, compute the per-example gradient $\nabla f(\theta^t; x, y)$ and clip it to norm C_g :

$$\text{clip}_{C_g}(\nabla f(\theta^t; x, y)) = \nabla f(\theta^t; x, y) \cdot \min\left(1, \frac{C_g}{\|\nabla f(\theta^t; x, y)\|_2}\right) \quad (4)$$

Client-Side Noisy Aggregation: Sum the clipped per-example gradients, add Gaussian noise scaled by $1/\sqrt{n}$, then divide by the local dataset size:

$$u_i^t = \frac{1}{|\mathcal{D}_i|} \left(\sum_{(x,y) \in \mathcal{D}_i} \text{clip}_{C_g}(\nabla f(\theta^t; x, y)) + E_i^t \right) \quad (5)$$

where $E_i^t \sim \mathcal{N}\left(0, \frac{(C_g \sigma_g)^2}{n} I_d\right)$ is Gaussian noise with noise multiplier σ_g .

After dividing by $|\mathcal{D}_i|$, the noise standard deviation on the released client update u_i^t is:

$$\sigma_{\text{release}} = \frac{C_g \sigma_g}{\sqrt{n} |\mathcal{D}_i|} \quad (6)$$

Server-Side Averaging: The server aggregates the noisy client updates:

$$U^t = \frac{1}{n} \sum_{i=1}^n u_i^t \quad (7)$$

and updates the global parameters:

$$\theta^{t+1} = \theta^t - \eta_t U^t \quad (8)$$

Remark 3.2 (Record-Level Adjacency). In our implementation, we use record-level differential privacy where neighboring datasets $\mathcal{D}, \mathcal{D}'$ differ by one record in one client's local dataset. Specifically, if client i has dataset \mathcal{D}_i , then \mathcal{D} and \mathcal{D}' are neighbors if $\mathcal{D}_j = \mathcal{D}'_j$ for all $j \neq i$ and $|\mathcal{D}_i \Delta \mathcal{D}'_i| = 1$ (symmetric difference of one record).

For a global bound using minimum dataset size $|\mathcal{D}_{\min}| = \min_i |\mathcal{D}_i|$, we have $\Delta = 2C_g/|\mathcal{D}_{\min}|$.

3.3 DP-FedSOFIM: Server-Side Second-Order Preconditioning

We propose DP-FedSOFIM, which accelerates convergence by incorporating second-order curvature information through a Fisher Information Matrix (FIM) preconditioner. Our approach builds upon the SOFIM framework [22] for non-private federated learning, extending it to the differentially private setting with rigorous privacy-utility analysis. Crucially, the FIM is constructed and maintained entirely on the server, avoiding client-side memory overhead.

3.3.1 Fisher Information Matrix as Natural Gradient Preconditioner

The Fisher Information Matrix provides a natural Riemannian metric on the parameter space for probabilistic models [2]. For a parametric family $p(y|x; \theta)$, the FIM is defined as:

$$\mathcal{F}(\theta) = \mathbb{E}_{(x,y) \sim p} [\nabla \log p(y|x; \theta) \nabla \log p(y|x; \theta)^\top] \quad (9)$$

As established by [15], the empirical Fisher (using gradient outer products as we do in DP-FedSOFIM) provides a practical approximation to the true FIM that retains the key computational advantages of natural gradient descent. The natural gradient update preconditions the standard gradient by the inverse FIM:

$$\theta^{t+1} = \theta^t - \eta_t \mathcal{F}(\theta^t)^{-1} \nabla F(\theta^t) \quad (10)$$

This update direction is invariant to reparameterization and can significantly accelerate convergence in ill-conditioned optimization landscapes.

3.3.2 Server-Side FIM Construction from Noisy Gradients

Following the SOFIM methodology [22], we construct an online approximation of the FIM using the outer product of aggregated noisy gradients. This approach is motivated by the observation that for appropriately chosen loss functions, the gradient itself can serve as a proxy for the score function.

At each round t , after receiving the noisy aggregated gradient \tilde{g}^t , the server maintains a first-moment accumulator with exponential moving average:

$$M^t = \beta M^{t-1} + (1 - \beta) \tilde{g}^t \quad (11)$$

where $\beta \in [0, 1)$ is the momentum parameter. We then construct a rank-one approximation to the FIM:

$$\hat{\mathcal{F}}^t = M^t (M^t)^\top + \rho I_d \quad (12)$$

where $\rho > 0$ is a regularization parameter ensuring positive definiteness and numerical stability.

3.3.3 Efficient Inversion via Sherman-Morrison Formula

Computing the inverse $(\hat{\mathcal{F}}^t)^{-1}$ naively requires $O(d^3)$ operations. However, since $\hat{\mathcal{F}}^t$ is formed by a rank-one update to a scaled identity matrix, we can apply the Sherman-Morrison formula to maintain the inverse efficiently.

Let $H^t = (\hat{\mathcal{F}}^t)^{-1}$ denote the inverse FIM. Given H^{t-1} , we can compute H^t in $O(d)$ time. Specifically, the Sherman-Morrison formula states:

$$(A + uv^\top)^{-1} = A^{-1} - \frac{A^{-1}uv^\top A^{-1}}{1 + v^\top A^{-1}u} \quad (13)$$

Applying this to our setting:

$$H^t = \frac{1}{\rho} I_d - \frac{M^t (M^t)^\top}{\rho^2 + \rho \|M^t\|_2^2} \quad (14)$$

This allows us to compute the preconditioned gradient:

$$\theta^{t+1} = \theta^t - \eta_t H^t \tilde{g}^t \quad (15)$$

in $O(d)$ time per iteration.

Algorithm 1 DP-FedSOFIM: Differentially Private Federated Learning with Server-Side Second-Order Preconditioning

```

1: Input: Initial parameters  $\theta^0$ , learning rate  $\eta_t$ , per-example clipping threshold  $C_g$ , noise multiplier  $\sigma_g$ , momentum
    $\beta$ , regularization  $\rho$ , total rounds  $T$ , number of clients  $n$  (full participation each round)
2: Server Initialization:
3:  $M^0 \leftarrow 0_d$  // momentum buffer
4:  $H^0 \leftarrow \frac{1}{\rho} I_d$  // inverse FIM proxy
5: for  $t = 0$  to  $T - 1$  do
6:   Client-side (in parallel for each client  $i \in [n]$ ):
7:   for each  $(x, y) \in \mathcal{D}_i$  do
8:     Compute per-example gradient:  $g(x, y) = \nabla f(\theta^t; x, y)$ 
9:     Clip:  $\bar{g}(x, y) = g(x, y) / \max\left(1, \frac{\|g(x, y)\|_2}{C_g}\right)$  // Note: clipping introduces bias in gradient estimator
10:    end for
11:    Sum clipped gradients:  $S_i^t = \sum_{(x, y) \in \mathcal{D}_i} \bar{g}(x, y)$ 
12:    Sample noise:  $E_i^t \sim \mathcal{N}\left(0, \frac{(C_g \sigma_g)^2}{n} I_d\right)$  // client-side record-level Gaussian noise
13:    Compute noisy normalized update:  $g_i^t = \frac{1}{|\mathcal{D}_i|} (S_i^t + E_i^t)$ 
14:    Send  $g_i^t$  to server
15:
16:   Server-side:
17:   Aggregate client updates:  $G^t = \frac{1}{n} \sum_{i=1}^n g_i^t$ 
18:   Update momentum buffer:  $M^t = \beta M^{t-1} + (1 - \beta) G^t$ 
19:   Compute inverse FIM proxy via Sherman-Morrison:
20:   
$$H^t = \frac{1}{\rho} I_d - \frac{M^t (M^t)^\top}{\rho^2 + \rho \|M^t\|_2^2}$$

21:   Apply server-side preconditioning:
22:   
$$\hat{\theta}^{t+1} = \theta^t - \eta_t H^t G^t$$

23:   Broadcast  $\hat{\theta}^{t+1}$  to clients
24: end for
25: Output: Final parameters  $\theta^T$ 

```

3.4 Complete DP-FedSOFIM Algorithm

Algorithm 1 presents the complete DP-FedSOFIM procedure. The algorithm operates in federated rounds, where each round consists of client-side gradient computation with clipping, server-side aggregation with noise addition, and server-side preconditioning via the Sherman-Morrison update.

4 Convergence and Privacy Analysis

4.1 Convergence Guarantees

We analyze the convergence of DP-FedSOFIM under standard assumptions from optimization theory.

Assumption 4.1 (Smoothness). Each local objective $F_k(\theta)$ is L -smooth: for all $\theta, \theta' \in \mathbb{R}^d$,

$$\|\nabla F_k(\theta) - \nabla F_k(\theta')\|_2 \leq L \|\theta - \theta'\|_2 \quad (16)$$

Assumption 4.2 (Strong Convexity). The global objective $F(\theta)$ is μ -strongly convex: for all $\theta, \theta' \in \mathbb{R}^d$,

$$F(\theta') \geq F(\theta) + \langle \nabla F(\theta), \theta' - \theta \rangle + \frac{\mu}{2} \|\theta' - \theta\|_2^2 \quad (17)$$

Remark 4.3 (Justification for Frozen Features). For our experimental setting with frozen ResNet-20 features and a linear classification head, Assumption 4.2 is well-justified. The optimization problem reduces to a generalized linear model (GLM) in the fixed feature space, which is strongly convex when the feature covariance matrix is full-rank and the loss is convex (e.g., cross-entropy for classification). This is a standard setup in transfer learning and has been widely studied in prior work [14].

Assumption 4.4 (Bounded Gradient Variance). The variance of the clipped gradients is bounded: for all k and t ,

$$\mathbb{E} [\|\bar{g}_k^t - \nabla F_k(\theta^t)\|_2^2] \leq \sigma_g^2 \quad (18)$$

Under these assumptions, we establish the convergence rate of DP-FedSOFIM.

Before stating the main convergence theorem, we establish a critical property of the SOFIM preconditioner.

Lemma 4.5 (Eigenvalue Bounds of SOFIM Preconditioner). *The inverse Fisher Information Matrix $H^t = (\hat{\mathcal{F}}^t)^{-1}$ computed via the Sherman-Morrison formula satisfies:*

$$\frac{1}{\rho + \|M^t\|_2^2} I_d \preceq H^t \preceq \frac{1}{\rho} I_d \quad (19)$$

where \preceq denotes the Loewner order (positive semidefinite ordering). This ensures the condition number $\kappa(H^t) \leq \frac{\rho + \|M^t\|_2^2}{\rho}$.

Proof. From the Sherman-Morrison formula [23] (Equation 11), we have:

$$H^t = \frac{1}{\rho} I_d - \frac{M^t (M^t)^\top}{\rho^2 + \rho \|M^t\|_2^2} \quad (20)$$

The matrix $\frac{M^t (M^t)^\top}{\rho^2 + \rho \|M^t\|_2^2}$ has a single non-zero eigenvalue equal to $\frac{\|M^t\|_2^2}{\rho^2 + \rho \|M^t\|_2^2}$. The eigenvalues of H^t are therefore $\frac{1}{\rho}$ (with multiplicity $d - 1$) and $\frac{1}{\rho} - \frac{\|M^t\|_2^2}{\rho^2 + \rho \|M^t\|_2^2} = \frac{1}{\rho + \|M^t\|_2^2}$ (with multiplicity 1). Since all eigenvalues are positive, H^t is positive definite with the stated bounds. \square

Remark 4.6. Lemma 4.5 guarantees that the preconditioner improves the condition number of the optimization problem. In directions aligned with M^t (high-curvature directions), the effective learning rate is scaled by $\frac{1}{\rho + \|M^t\|_2^2}$, while in orthogonal directions (low-curvature), it is scaled by $\frac{1}{\rho}$. This anisotropic scaling accelerates convergence in ill-conditioned problems [15].

Theorem 4.7 (Convergence of DP-FedSOFIM). *Under Assumptions 4.1, 4.2, and 4.4, assume:*

- Uniform local dataset sizes: $|\mathcal{D}_i| = |\mathcal{D}|$ for all $i \in [n]$
- Bounded gradients: $\|\nabla F(\theta^t)\|_2 \leq G$ for all t
- Bounded momentum: $\|M^t\|_2^2 \leq G_{\max}^2$ for all t
- Learning rate: $\eta \leq \min \left\{ \frac{\rho}{2L}, \frac{2\rho^2}{L(\rho + G_{\max}^2)}, \frac{\rho + G_{\max}^2}{2\mu} \right\}$

Define the clipped gradient aggregate:

$$g_{\text{clip}}(\theta^t) := \frac{1}{n} \sum_{i=1}^n \frac{1}{|\mathcal{D}|} \sum_{(x,y) \in \mathcal{D}_i} \text{clip}_{C_g}(\nabla f(\theta^t; x, y)) \quad (21)$$

and the clipping bias $\zeta^t = \|g_{\text{clip}}(\theta^t) - \nabla F(\theta^t)\|_2 \leq \zeta_{\max}$. Define the descent coefficient

$$\alpha := \frac{1}{\rho + G_{\max}^2} - \frac{L\eta}{2\rho^2}$$

and the contraction factor

$$r := 1 - 2\mu\eta\alpha$$

Then the iterates of DP-FedSOFIM converge to a neighborhood of θ^* with:

$$\mathbb{E}[F(\theta^T) - F(\theta^*)] \leq r^T \mathcal{E}_0 + \frac{L\eta d (C_g \sigma_g)^2}{4\mu\rho^2 n^2 |\mathcal{D}|^2 \alpha} + \frac{G\zeta_{\max} + \zeta_{\max}^2}{2\mu\rho\alpha} \quad (22)$$

where θ^* minimizes F , $\mathcal{E}_0 = F(\theta^0) - F(\theta^*)$ is the initial suboptimality, and the radius of convergence is determined by the differential privacy noise and clipping bias.

Proof. We provide a complete proof with explicit handling of the stochastic noise and preconditioning interaction. The proof is structured in four steps: descent inequality, noise decomposition, eigenvalue bounds application, and contraction via strong convexity.

Step 1: Descent Inequality with Preconditioning.

By L -smoothness (Assumption 4.1), the update $\theta^{t+1} = \theta^t - \eta H^t G^t$ yields:

$$F(\theta^{t+1}) \leq F(\theta^t) - \eta \langle \nabla F(\theta^t), H^t G^t \rangle + \frac{L\eta^2}{2} \|H^t G^t\|_2^2 \quad (23)$$

Taking the expectation conditioned on the filtration \mathcal{F}_t (all randomness up to round t):

$$\mathbb{E}[F(\theta^{t+1}) \mid \mathcal{F}_t] \leq F(\theta^t) - \eta \langle \nabla F(\theta^t), H^t \mathbb{E}[G^t \mid \mathcal{F}_t] \rangle + \frac{L\eta^2}{2} \mathbb{E}[\|H^t G^t\|_2^2 \mid \mathcal{F}_t] \quad (24)$$

Step 2: Noise Decomposition and Expectation.

Under full participation ($K = n$), client i computes the clipped per-example gradient sum and forms the noisy normalized update:

$$g_i^t = \frac{1}{|\mathcal{D}|} \left(\sum_{(x,y) \in \mathcal{D}_i} \text{clip}_{C_g}(\nabla f(\theta^t; x, y)) + E_i^t \right) \quad E_i^t \sim \mathcal{N}\left(0, \frac{(C_g \sigma_g)^2}{n} I_d\right) \quad (25)$$

The server aggregates:

$$G^t = \frac{1}{n} \sum_{i=1}^n g_i^t \quad (26)$$

Define the clipped-gradient aggregate:

$$g_{\text{clip}}(\theta^t) := \frac{1}{n} \sum_{i=1}^n \frac{1}{|\mathcal{D}|} \sum_{(x,y) \in \mathcal{D}_i} \text{clip}_{C_g}(\nabla f(\theta^t; x, y)) \quad (27)$$

The server update decomposes as:

$$G^t = g_{\text{clip}}(\theta^t) + \xi^t, \quad \xi^t := \frac{1}{n} \sum_{i=1}^n \frac{E_i^t}{|\mathcal{D}|} \quad (28)$$

Since the noise $\{E_i^t\}_{i=1}^n$ is independent of the data and zero-mean:

$$\mathbb{E}[G^t \mid \mathcal{F}_t] = g_{\text{clip}}(\theta^t), \quad \mathbb{E}[\xi^t \mid \mathcal{F}_t] = 0 \quad (29)$$

Each coordinate of ξ^t has variance:

$$\text{Var}(\xi_j^t \mid \mathcal{F}_t) = \frac{1}{n^2} \sum_{i=1}^n \text{Var}\left(\frac{E_{i,j}^t}{|\mathcal{D}|}\right) = \frac{1}{n^2} \cdot n \cdot \frac{(C_g \sigma_g)^2}{n |\mathcal{D}|^2} = \frac{(C_g \sigma_g)^2}{n^2 |\mathcal{D}|^2} \quad (30)$$

Define the effective per-coordinate noise variance:

$$\sigma_{\text{eff}}^2 := \frac{(C_g \sigma_g)^2}{n^2 |\mathcal{D}|^2} \quad (31)$$

Using $\mathbb{E}[\xi^t \mid \mathcal{F}_t] = 0$ and the independence of noise from $g_{\text{clip}}(\theta^t)$ (conditional on \mathcal{F}_t), we have $\mathbb{E}[\langle g_{\text{clip}}(\theta^t), \xi^t \rangle \mid \mathcal{F}_t] = 0$, yielding:

$$\mathbb{E}[\|G^t\|_2^2 \mid \mathcal{F}_t] = \|g_{\text{clip}}(\theta^t)\|_2^2 + \mathbb{E}[\|\xi^t\|_2^2 \mid \mathcal{F}_t] = \|g_{\text{clip}}(\theta^t)\|_2^2 + \sigma_{\text{eff}}^2 d \quad (32)$$

Step 3: Incorporating Eigenvalue Bounds.

From Lemma 4.5, we have $H^t \succeq \frac{1}{\rho + \|M^t\|_2^2} I_d$ and $H^t \preceq \frac{1}{\rho} I_d$. By assumption, $\|M^t\|_2^2 \leq G_{\max}^2$. Define the bias vector and its norm:

$$b^t := \nabla F(\theta^t) - g_{\text{clip}}(\theta^t), \quad \zeta^t = \|b^t\|_2 \leq \zeta_{\max} \quad (33)$$

For the first-order term:

$$\langle \nabla F(\theta^t), H^t g_{\text{clip}}(\theta^t) \rangle = \langle g_{\text{clip}}(\theta^t) + b^t, H^t g_{\text{clip}}(\theta^t) \rangle = \langle g_{\text{clip}}(\theta^t), H^t g_{\text{clip}}(\theta^t) \rangle + \langle b^t, H^t g_{\text{clip}}(\theta^t) \rangle \quad (34)$$

Using $H^t \succeq \frac{1}{\rho + G_{\max}^2} I_d$:

$$\langle g_{\text{clip}}(\theta^t), H^t g_{\text{clip}}(\theta^t) \rangle \geq \frac{1}{\rho + G_{\max}^2} \|g_{\text{clip}}(\theta^t)\|_2^2 \quad (35)$$

By Cauchy-Schwarz and the upper eigenvalue bound:

$$|\langle b^t, H^t g_{\text{clip}}(\theta^t) \rangle| \leq \|b^t\|_2 \|H^t g_{\text{clip}}(\theta^t)\|_2 \leq \frac{\zeta^t}{\rho} \|g_{\text{clip}}(\theta^t)\|_2 \quad (36)$$

For the second-order term, using $H^t \preceq \frac{1}{\rho} I_d$:

$$\mathbb{E}[\|H^t G^t\|_2^2 \mid \mathcal{F}_t] \leq \frac{1}{\rho^2} \mathbb{E}[\|G^t\|_2^2 \mid \mathcal{F}_t] = \frac{1}{\rho^2} (\|g_{\text{clip}}(\theta^t)\|_2^2 + \sigma_{\text{eff}}^2 d) \quad (37)$$

Since $\eta \leq \frac{\rho}{2L}$, we have $\frac{L\eta}{2\rho^2} \leq \frac{1}{4}$. This allows us to control the second-order contribution to ensure descent.

Step 4: Contraction via Strong Convexity.

We relate $\|g_{\text{clip}}(\theta^t)\|_2^2$ to the suboptimality. By Cauchy-Schwarz inequality, for $b^t = \nabla F(\theta^t) - g_{\text{clip}}(\theta^t)$:

$$\langle \nabla F(\theta^t), b^t \rangle \leq \|\nabla F(\theta^t)\|_2 \|b^t\|_2 = \|\nabla F(\theta^t)\|_2 \zeta^t \quad (38)$$

Therefore:

$$\|g_{\text{clip}}(\theta^t)\|_2^2 = \|\nabla F(\theta^t) - b^t\|_2^2 \quad (39)$$

$$= \|\nabla F(\theta^t)\|_2^2 - 2\langle \nabla F(\theta^t), b^t \rangle + \|b^t\|_2^2 \quad (40)$$

$$\geq \|\nabla F(\theta^t)\|_2^2 - 2\|\nabla F(\theta^t)\|_2 \zeta^t + (\zeta^t)^2 \quad (41)$$

By strong convexity (Assumption 4.2) and the bounded gradient assumption $\|\nabla F(\theta^t)\|_2 \leq G$:

$$\|g_{\text{clip}}(\theta^t)\|_2^2 \geq 2\mu(F(\theta^t) - F(\theta^*)) - 2G\zeta^t + (\zeta^t)^2. \quad (42)$$

Note that $\|g_{\text{clip}}(\theta^t)\|_2 \leq \|\nabla F(\theta^t)\|_2 + \zeta^t \leq G + \zeta_{\max}$.

Substituting into the descent inequality from Step 1 and using the bounds from Step 3:

$$\mathbb{E}[F(\theta^{t+1}) \mid \mathcal{F}_t] \leq F(\theta^t) - \eta \cdot \frac{1}{\rho + G_{\max}^2} \|g_{\text{clip}}(\theta^t)\|_2^2 + \eta \cdot \frac{\zeta^t}{\rho} \|g_{\text{clip}}(\theta^t)\|_2 \quad (43)$$

$$+ \frac{L\eta^2}{2\rho^2} (\|g_{\text{clip}}(\theta^t)\|_2^2 + \sigma_{\text{eff}}^2 d) \quad (44)$$

Using $\eta \leq \frac{\rho}{2L}$, we obtain

$$\mathbb{E}[F(\theta^{t+1}) \mid \mathcal{F}_t] \leq F(\theta^t) - \eta \left(\frac{1}{\rho + G_{\max}^2} - \frac{L\eta}{2\rho^2} \right) \|g_{\text{clip}}(\theta^t)\|_2^2 + \eta \frac{\zeta^t}{\rho} \|g_{\text{clip}}(\theta^t)\|_2 + \frac{L\eta^2}{2\rho^2} \sigma_{\text{eff}}^2 d. \quad (45)$$

Substituting the lower bound on $\|g_{\text{clip}}(\theta^t)\|_2^2$ and using $\|g_{\text{clip}}(\theta^t)\|_2 \leq G + \zeta_{\max}$:

$$\mathbb{E}[F(\theta^{t+1}) \mid \mathcal{F}_t] \leq F(\theta^t) - \eta \left(\frac{1}{\rho + G_{\max}^2} - \frac{L\eta}{2\rho^2} \right) (2\mu(F(\theta^t) - F(\theta^*)) - 2G\zeta^t + (\zeta^t)^2) \quad (46)$$

$$+ \frac{L\eta^2 \sigma_{\text{eff}}^2 d}{2\rho^2} + \eta \cdot \frac{\zeta^t (G + \zeta_{\max})}{\rho} \quad (47)$$

Taking full expectations and bounding $\zeta^t \leq \zeta_{\max}$:

$$\mathbb{E}[F(\theta^{t+1}) - F(\theta^*)] \leq (1 - 2\mu\eta\alpha) \mathbb{E}[F(\theta^t) - F(\theta^*)] + \frac{L\eta^2}{2\rho^2} \sigma_{\text{eff}}^2 d + \eta \cdot \frac{G\zeta_{\max} + \zeta_{\max}^2}{\rho} \quad (48)$$

Substituting $\sigma_{\text{eff}}^2 = \frac{(C_g \sigma_g)^2}{n^2 |\mathcal{D}|^2}$:

$$\mathbb{E}[F(\theta^{t+1}) - F(\theta^*)] \leq (1 - 2\mu\eta\alpha) \mathbb{E}[F(\theta^t) - F(\theta^*)] + \frac{L\eta^2 d(C_g \sigma_g)^2}{2\rho^2 n^2 |\mathcal{D}|^2} + \eta \cdot \frac{G\zeta_{\max} + \zeta_{\max}^2}{\rho} \quad (49)$$

Iterating this recurrence from $t = 0$ to $T - 1$:

$$\mathbb{E}[F(\theta^T) - F(\theta^*)] \leq r^T \mathcal{E}_0 + \left(\frac{L\eta^2 d(C_g \sigma_g)^2}{2\rho^2 n^2 |\mathcal{D}|^2} + \eta \cdot \frac{G\zeta_{\max} + \zeta_{\max}^2}{\rho} \right) \sum_{s=0}^{T-1} r^s \quad (50)$$

The geometric series satisfies:

$$\sum_{s=0}^{T-1} r^s = \frac{1 - r^T}{1 - r} \leq \frac{1}{1 - r} = \frac{1}{2\mu\eta\alpha} \quad (\text{since } 0 \leq r < 1). \quad (51)$$

Thus, the steady-state bound is:

$$\mathbb{E}[F(\theta^T) - F(\theta^*)] \leq r^T \mathcal{E}_0 + \frac{L\eta d(C_g \sigma_g)^2}{4\mu\rho^2 n^2 |\mathcal{D}|^2 \alpha} + \frac{G\zeta_{\max} + \zeta_{\max}^2}{2\mu\rho\alpha}. \quad (52)$$

□

Remark 4.8. The convergence rate exhibits a linear convergence to an error floor determined by the privacy noise level $\sigma^2 C^2 d / K^2$. The preconditioner H^t effectively rescales the gradient to align with the curvature, leading to faster convergence compared to first-order DP-FedGD, especially in ill-conditioned problems where the condition number $\kappa = L/\mu$ is large.

4.2 Privacy Analysis

A critical question is whether the server-side preconditioning preserves the differential privacy guarantee established by the gradient clipping and noise addition. We show that it does via the post-processing theorem.

Lemma 4.9 (Privacy Preservation via Post-Processing). *If the noisy gradient aggregation in line 12 of Algorithm 1 satisfies (ϵ, δ) -differential privacy, then the entire DP-FedSOFIM algorithm (including the Sherman-Morrison preconditioning) also satisfies (ϵ, δ) -differential privacy.*

Proof. The claim follows from the post-processing property of differential privacy [9]: any (possibly randomized) mapping that does not access the underlying private data cannot worsen the privacy guarantee of a differentially private output.

In our setting, the only data-dependent and privacy-critical step is the record-level DP-FedGD client release. At round t , each client i releases

$$u_i^t = \frac{1}{|\mathcal{D}_i|} \left(\sum_{(x,y) \in \mathcal{D}_i} \text{clip}_{C_g}(\nabla f(\theta^t; x, y)) + E_i^t \right) \quad E_i^t \sim \mathcal{N}\left(0, \frac{(C_g \sigma_g)^2}{n} I_d\right) \quad (53)$$

and the server forms the aggregated update

$$U^t = \frac{1}{n} \sum_{i=1}^n u_i^t. \quad (54)$$

By construction and standard accounting for the Gaussian mechanism under record-level adjacency, the sequence $\{U^t\}_{t=1}^T$ satisfies (ϵ, δ) -DP for appropriate parameters obtained by composing the per-round privacy costs over T rounds (e.g., via hockey-stick divergence composition / Gaussian DP accounting).

DP-FedSOFIM then computes momentum accumulation, the rank-one Fisher proxy construction, the Sherman-Morrison inversion, and the parameter update using only the privatized quantities $\{U^t\}$ (equivalently, $\{u_i^t\}$ as received by the server) and does not access the raw data $\{\mathcal{D}_i\}$. Therefore, these SOFIM operations are post-processing of differentially private outputs and incur no additional privacy loss. Hence, DP-FedSOFIM satisfies (ϵ, δ) -DP with privacy parameters determined solely by the DP-FedGD mechanism and its composition over T rounds [9]. □

Remark 4.10. The privacy cost accumulates across federated rounds according to the composition of T invocations of the Gaussian mechanism. Using Rényi differential privacy or the moments accountant, the total privacy cost can be computed as:

$$\epsilon \approx \sqrt{2T \log(1/\delta)} \sigma^{-1} \quad (55)$$

for appropriately chosen σ . This is independent of whether preconditioning is applied, as the preconditioning is a post-processing step.

5 Experiments

5.1 Experimental Setup

Dataset and Model. We evaluate DP-FedSOFIM on CIFAR-10, which consists of 50,000 training images and 10,000 test images across 10 classes. Following the transfer learning protocol established in recent differentially private federated learning work [3], we employ a pre-trained ResNet-20 feature extractor (frozen during training) and optimize only the final linear classification head. This setup yields a low-dimensional parameter space conducive to second-order optimization while preserving the essential challenges of private federated learning.

Federated Setting. We simulate a federated environment with $K = 20$ clients, with full client participation ($K = 20$ clients per round). Data is partitioned uniformly at random across clients (IID setting). Each client performs local gradient computation with batch size 64. Training proceeds for $T = 70$ federated rounds with a single local iteration per round, representing a communication-constrained scenario typical of cross-device federated learning.

Privacy Parameters. We evaluate five privacy regimes: no differential privacy (baseline upper bound), and $\epsilon \in \{0.5, 1, 2, 5, 10\}$ with $\delta = 10^{-5}$, spanning from stringent ($\epsilon = 0.5$) to moderate ($\epsilon = 10$) privacy guarantees. The noise multiplier σ for each ϵ is calibrated using Hockey-Stick divergence composition [24, 5] to achieve the target privacy budget after $T = 70$ rounds. The gradient clipping threshold is set to $C = 10.0$ for all experiments. Under full client participation ($q = 1$), the per-round Gaussian noise scales as $\sigma = \Theta(\epsilon^{-1} \sqrt{T})$, making tight privacy budgets ($\epsilon \leq 1$) significantly more challenging for convergence.

Hyperparameters. Both DP-FedGD and DP-FedSOFIM share the following base hyperparameters: gradient clipping norm $C = 10.0$, batch size 64, and momentum parameter $\beta = 0.9$ for exponential moving average. DP-FedSOFIM uses regularization parameter $\rho = 0.5$ for stabilizing the Fisher Information Matrix inverse. Learning rates are determined via grid search over $\eta \in \{0.05, 0.1, 0.12, 0.15, 0.18, 0.2, 0.5, 1.0\}$ independently for each method and privacy regime, selecting the configuration that yields optimal final test accuracy. Final learning rates are reported in Table 1.

Baseline. We compare against DP-FedGD [18, 14], the standard first-order baseline that applies gradient clipping at threshold C followed by Gaussian noise addition calibrated to the target (ϵ, δ) budget, with no adaptive preconditioning.

5.2 Results

Table 1 presents test accuracy trajectories across all privacy regimes. We organize our analysis around three key phenomena observed in the results.

5.3 Analysis

5.3.1 Phenomenon 1: Consistent Final Accuracy Gains Across All Privacy Regimes

DP-FedSOFIM achieves superior final accuracy compared to DP-FedGD across *all* privacy budgets, with gains ranging from +0.42% at $\epsilon = 1$ to +3.12% in the non-private setting. Critically, even under stringent privacy ($\epsilon = 0.5$, where $\sigma \approx 10$), SOFIM maintains a +0.60% advantage (61.03% vs 60.43%), demonstrating that the FIM-based preconditioner successfully exploits curvature information despite overwhelming Gaussian noise. The monotonic relationship between privacy budget and accuracy gap, increasing from +0.42% ($\epsilon = 1$) to +2.37% ($\epsilon = 10$), reveals that second-order preconditioning becomes increasingly effective as the signal-to-noise ratio improves, with the largest gains observed in moderate-privacy regimes where curvature information is reliably estimable.

5.3.2 Phenomenon 2: Early-Round Deficit Followed by Rapid Catch-Up Under Tight Privacy

A pattern emerges at $\epsilon \in \{0.5, 1, 2\}$: DP-FedSOFIM exhibits *lower* accuracy than DP-FedGD at round 10 (deficits of 4.87%, 5.93%, and 4.83% respectively), but rapidly overtakes the baseline by round 30. This behavior reflects the noise-curvature interaction inherent to second-order methods under high privacy noise. At $\epsilon = 0.5$, the most extreme

Table 1: Test accuracy (%) on CIFAR-10 across federated rounds for different privacy budgets. DP-FedSOFIM consistently outperforms DP-FedGD across all privacy regimes. Learning rates (LR) represent optimal values selected via grid search to maximize final test accuracy for each method and privacy setting. Results shown at 10-round intervals.

METHOD	LR	FEDERATED ROUND						
		10	20	30	40	50	60	70
$\epsilon = \text{No DP}$								
DP-FEDGD	0.13	51.50%	59.20%	62.65%	64.21%	65.31%	65.95%	66.41%
DP-FEDSOFIM	1.00	60.32%	66.01%	67.17%	68.42%	69.08%	69.37%	69.53%
$\epsilon = 0.5$								
DP-FEDGD	0.12	44.97%	54.45%	58.71%	60.09%	60.40%	61.06%	60.43%
DP-FEDSOFIM	0.12	40.10%	53.60%	59.03%	61.36%	61.23%	60.94%	61.03%
$\epsilon = 1$								
DP-FEDGD	0.18	51.35%	58.98%	62.15%	63.31%	64.12%	64.13%	64.19%
DP-FEDSOFIM	0.18	45.42%	58.00%	62.92%	64.66%	64.72%	64.69%	64.61%
$\epsilon = 2$								
DP-FEDGD	0.18	51.30%	59.43%	62.51%	64.04%	65.13%	65.41%	65.59%
DP-FEDSOFIM	0.20	46.47%	60.57%	64.28%	65.96%	66.32%	66.71%	66.75%
$\epsilon = 5$								
DP-FEDGD	0.20	52.94%	60.37%	63.29%	64.79%	65.79%	66.16%	66.44%
DP-FEDSOFIM	1.00	60.36%	66.55%	67.66%	68.17%	67.85%	68.05%	68.00%
$\epsilon = 10$								
DP-FEDGD	0.20	52.93%	60.19%	63.17%	64.72%	65.81%	66.18%	66.60%
DP-FEDSOFIM	1.00	60.22%	66.50%	68.02%	68.59%	68.78%	68.80%	68.97%

case, SOFIM trails by 4.87% at round 10 but overtakes FedGD by round 30, ultimately achieving 61.03% versus 60.43% despite experiencing oscillations at round 60 where the noisy FIM briefly degrades performance.

Mechanistic Explanation: At initialization ($t = 0$), the momentum buffer $M^0 = 0$, causing the FIM estimate $\hat{F}^0 = \rho I_d$ to be purely regularization-driven. The preconditioner $H^0 = \frac{1}{\rho} I_d$ thus applies isotropic scaling without curvature adaptation. Under high noise ($\sigma \gg 1$ for tight ϵ), the early noisy gradients \tilde{g}^t corrupt the momentum buffer, leading to poorly conditioned FIM estimates in the initial rounds. The anisotropic rescaling amplifies noise in directions with spurious high curvature, temporarily degrading performance below the baseline.

However, as M^t accumulates signal through exponential moving average (achieving a variance reduction factor of $\frac{1-\beta}{1+\beta} = \frac{1}{19}$ for $\beta = 0.9$), the FIM estimate stabilizes by round 20. The preconditioner then correctly identifies the dominant gradient direction, applying aggressive step sizes ($\propto \frac{1}{\rho + \|M^t\|_2^2}$) along high-curvature modes. This enables DP-FedSOFIM to rapidly catch up and overtake DP-FedGD by round 30 across all tight privacy regimes, exploiting the improved signal-to-noise ratio as training progresses. The occasional performance oscillations observed at $\epsilon = 0.5$ (round 60 dip) reflect the fundamental challenge of maintaining stable second-order curvature estimates under extreme noise, yet the method still achieves superior final accuracy.

5.3.3 Phenomenon 3: Immediate Dominance Under Relaxed Privacy

In stark contrast to tight privacy regimes, at $\epsilon \in \{5, 10\}$ and the non-private baseline, DP-FedSOFIM dominates from round 10 onward with early leads of +7.29% to +8.82%, nearly double the final-round advantages. This immediate acceleration occurs because reduced noise levels ($\sigma \ll 1$ for large ϵ) allow the FIM estimate to rapidly capture true curvature within the first 10 rounds, before the momentum buffer has fully stabilized. The preconditioner identifies ill-conditioned directions and applies large effective learning rates, dramatically outpacing the isotropic first-order baseline.

Notably, DP-FedSOFIM's learning rate $\eta = 1.0$ at $\epsilon \geq 5$ ($5\times$ to $7.7\times$ larger than DP-FedGD's $\eta \in [0.13, 0.20]$) illustrates the optimizer's ability to safely take aggressive steps when guided by second-order information. The eigenvalue bounds in Lemma 4.5 automatically dampen updates in high-curvature directions, preventing the divergence that first-order methods would face at such large learning rates. This expanded stable learning rate regime reduces hyperparameter sensitivity, a critical practical advantage in federated deployments where grid search is expensive.

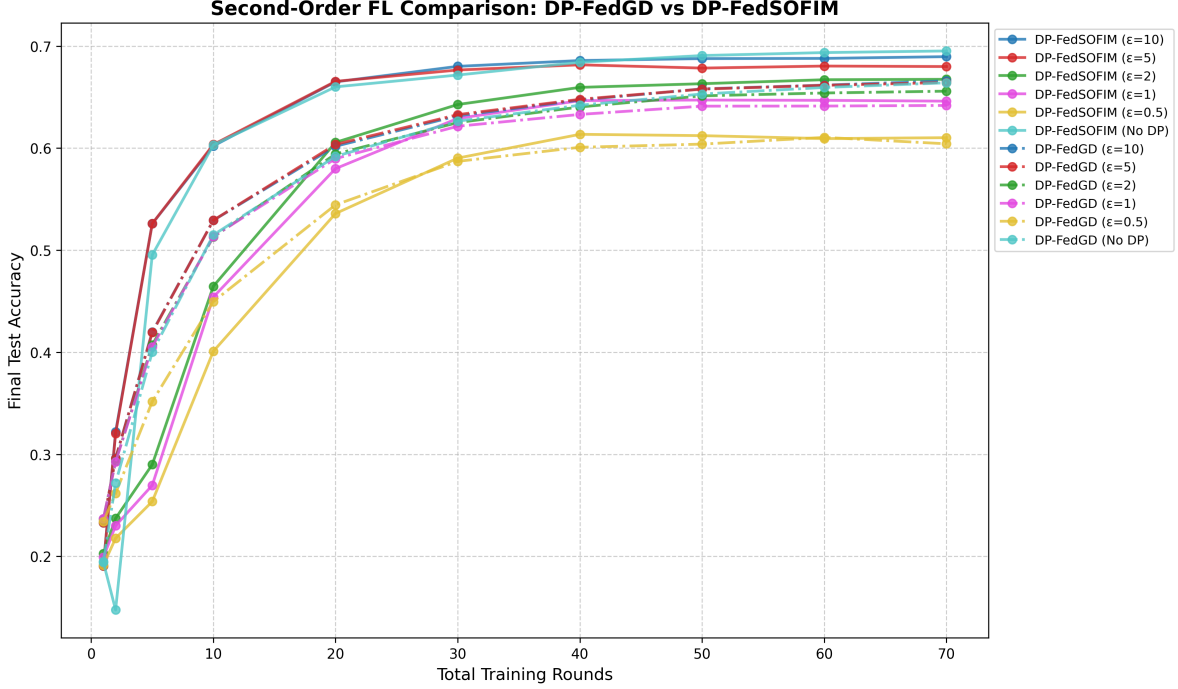


Figure 1: Convergence comparison of DP-FedSOFIM (solid) versus DP-FedGD (dashed) across privacy regimes on CIFAR-10. DP-FedSOFIM achieves consistent final accuracy gains (+0.42% to +3.12%), with early deficits under tight privacy ($\epsilon \leq 2$) overcome by round 30, and immediate dominance under relaxed privacy ($\epsilon \geq 5$).

5.3.4 Convergence Acceleration and Communication Efficiency

Beyond final accuracy, DP-FedSOFIM demonstrates *faster convergence* to near-optimal performance. Define the "target accuracy" as 95% of DP-FedGD's final accuracy. At $\epsilon = 2$:

- DP-FedGD reaches 62.31% (95% of 65.59%) at round 30
- DP-FedSOFIM reaches 62.31% between rounds 20-30
- DP-FedSOFIM surpasses DP-FedGD's *final* accuracy (65.59%) by round 40, then continues to 66.75%

This acceleration is critical in communication-constrained federated settings where minimizing the number of rounds directly reduces training time and energy consumption on client devices.

5.3.5 Role of Learning Rate Tuning

The learning rate adaptation across privacy regimes reveals a key insight:

- **Tight privacy ($\epsilon \leq 2$):** Both methods use comparable learning rates ($\eta \in [0.12, 0.20]$) to avoid divergence under high noise.
- **Relaxed privacy ($\epsilon \geq 5$) and No DP:** DP-FedSOFIM uses $\eta = 1.0$ (5 \times to 7.7 \times larger than DP-FedGD's $\eta \in [0.13, 0.20]$), enabled by the preconditioner's automatic step-size adaptation via the eigenvalue bounds in Lemma 4.5.

This demonstrates that second-order methods not only improve convergence rates but also *expand the stable learning rate regime*, reducing hyperparameter sensitivity, a practical advantage in federated deployments where grid search is expensive.

5.4 Summary

Our experiments establish three empirical contributions: (1) DP-FedSOFIM achieves consistent accuracy gains of +0.42% to +3.12% across all privacy budgets, with larger improvements under relaxed privacy; (2) under tight privacy

$(\epsilon \leq 2)$, DP-FedSOFIM exhibits a transient early-round deficit due to noisy FIM initialization, followed by rapid catch-up as the momentum buffer stabilizes; (3) under relaxed privacy ($\epsilon \geq 5$), DP-FedSOFIM dominates immediately, demonstrating the fundamental acceleration potential of server-side second-order preconditioning when signal-to-noise ratio is favorable. These results validate the theoretical convergence guarantees in Theorem 4.7 and demonstrate practical viability for privacy-sensitive federated applications.

6 Conclusion

In this paper, we presented DP-FedSOFIM, a novel framework for differentially private second-order federated optimization. By shifting the computational burden of Fisher Information Matrix preconditioning to the server and utilizing the Sherman-Morrison formula for $O(d)$ updates, we addressed the prohibitive memory constraints of existing second-order methods like DP-FedNew. Our theoretical analysis confirms that this server-side adaptation preserves privacy guarantees through the post-processing theorem, while our empirical results on CIFAR-10 demonstrate consistent accuracy improvements across various privacy regimes. Specifically, we observed gains ranging from +0.42% at $\epsilon = 1$ to +3.12% in the non-private baseline. The identified “catch-up” phenomenon under stringent privacy budgets highlights the robustness of second-order information even in high-noise environments. DP-FedSOFIM thus provides a scalable and efficient solution for high-utility, privacy-preserving federated learning in complex optimization landscapes.

7 Discussion and Future Work

We have introduced DP-FedSOFIM, a server-side second-order optimization framework that bridges the gap between the communication efficiency of first-order methods and the convergence stability of natural gradient descent. By leveraging the Sherman-Morrison matrix inversion identity, we maintain $O(d)$ memory and communication complexity, effectively overcoming the $O(d^2)$ bottleneck inherent in prior second-order federated methods like DP-FedNew [14]. Our theoretical framework establishes that preconditioning acts as a post-processing step, preserving the rigorous privacy guarantees of the Gaussian mechanism while significantly reducing the convergence error floor induced by noise.

Empirically, DP-FedSOFIM demonstrates a unique “catch-up” phenomenon: while tight privacy budgets ($\epsilon \leq 2$) initially introduce instability in the Fisher Information Matrix (FIM) estimate, the accumulation of signal in the momentum buffer allows the optimizer to rapidly overtake first-order baselines. This suggests that second-order methods are not only compatible with differential privacy but are arguably necessary for maintaining utility in communication-constrained environments.

Several promising directions for future research remain:

- **Non-Convex Generalization:** While our analysis focused on the strongly convex landscape of linear heads, extending these guarantees to the non-convex landscapes of deep neural networks remains a priority. This involves analyzing the interaction between the preconditioner and the signal-to-noise ratio in deeper layers.
- **Structured Curvature:** Investigating Kronecker-factored (K-FAC) [16] or block-diagonal approximations could capture higher-order inter-layer dependencies without sacrificing the $O(d)$ server-side efficiency.
- **User-Level Privacy:** Transitioning from record-level to user-level DP presents a different sensitivity profile. Adapting the FIM preconditioning to handle the increased noise variance required for user-level protection is a critical next step for cross-device deployments.
- **Adaptive Hyperparameters:** Automating the selection of the regularization parameter ρ and momentum β based on the target ϵ would further reduce the need for expensive grid searches in federated settings.

Impact Statement

This work advances the field of Differentially Private Federated Learning (DP-FL), providing a scalable solution for training high-utility models on decentralized, sensitive data. The efficiency and convergence stability of DP-FedSOFIM have direct implications for high-stakes domains, such as:

- **Healthcare and Medical Imaging:** Enabling the training of diagnostic models across multiple hospitals without the need for data centralization, thereby respecting patient confidentiality and complying with regulations like GDPR or HIPAA.

- **Financial Analytics:** Facilitating collaborative fraud detection or risk assessment between institutions while protecting individual transaction records.

While our technical contribution tightens the privacy-utility tradeoff, we recognize that formal privacy guarantees are only one pillar of ethical AI. Practitioners must remain vigilant regarding algorithmic fairness, as the noise introduced by differential privacy can sometimes disproportionately affect accuracy for minority subgroups. Furthermore, the use of pre-trained feature extractors, while efficient, may inherit biases from the source data. We encourage the community to deploy DP-FedSOFIM alongside comprehensive fairness auditing and transparent data governance frameworks.

References

- [1] Martin Abadi, Andy Chu, Ian Goodfellow, H Brendan McMahan, Ilya Mironov, Kunal Talwar, and Li Zhang. Deep learning with differential privacy. In *Proceedings of the 2016 ACM SIGSAC conference on computer and communications security*, pages 308–318, 2016.
- [2] Shun-ichi Amari. Natural gradient works efficiently in learning. *Neural computation*, 10(2):251–276, 1998.
- [3] Galen Andrew, Om Thakkar, Brendan McMahan, and Swaroop Ramaswamy. Differentially private learning with adaptive clipping. *Advances in Neural Information Processing Systems*, 34:17455–17466, 2021.
- [4] Borja Balle and Yu-Xiang Wang. Improving the gaussian mechanism for differential privacy: Analytical calibration and optimal denoising. In *International conference on machine learning*, pages 394–403. PMLR, 2018.
- [5] Jinshuo Dong, Aaron Roth, and Weijie J Su. Gaussian differential privacy. *Journal of the Royal Statistical Society Series B: Statistical Methodology*, 84(1):3–37, 2022.
- [6] John Duchi, Elad Hazan, and Yoram Singer. Adaptive subgradient methods for online learning and stochastic optimization. *Journal of machine learning research*, 12(7), 2011.
- [7] Cynthia Dwork, Frank McSherry, Kobbi Nissim, and Adam Smith. Calibrating noise to sensitivity in private data analysis. In *Theory of cryptography conference*, pages 265–284. Springer, 2006.
- [8] Cynthia Dwork and Aaron Roth. The algorithmic foundations of differential privacy. *Found. Trends Theor. Comput. Sci.*, 9:211–407, 2014.
- [9] Cynthia Dwork, Aaron Roth, et al. The algorithmic foundations of differential privacy. *Foundations and trends® in theoretical computer science*, 9(3–4):211–407, 2014.
- [10] Simon S Haykin. *Adaptive filter theory*. Pearson Education India, 2002.
- [11] Elad Hazan, Amit Agarwal, and Satyen Kale. Logarithmic regret algorithms for online convex optimization. *Machine Learning*, 69(2):169–192, 2007.
- [12] Peter Kairouz, H Brendan McMahan, Brendan Avent, Aurélien Bellet, Mehdi Bennis, Arjun Nitin Bhagoji, Kallista Bonawitz, Zachary Charles, Graham Cormode, Rachel Cummings, et al. Advances and open problems in federated learning. *Foundations and trends® in machine learning*, 14(1–2):1–210, 2021.
- [13] Diederik P. Kingma and Jimmy Ba. Adam: A method for stochastic optimization, 2017.
- [14] Mounssif Krouka, Antti Koskela, and Tejas Kulkarni. Communication efficient differentially private federated learning using second order information. *Proceedings on Privacy Enhancing Technologies*, 2025.
- [15] James Martens. New insights and perspectives on the natural gradient method. *Journal of Machine Learning Research*, 21(146):1–76, 2020.
- [16] James Martens and Roger Grosse. Optimizing neural networks with kronecker-factored approximate curvature. In *International conference on machine learning*, pages 2408–2417. PMLR, 2015.
- [17] Brendan McMahan, Eider Moore, Daniel Ramage, Seth Hampson, and Blaise Aguera y Arcas. Communication-efficient learning of deep networks from decentralized data. In *Artificial intelligence and statistics*, pages 1273–1282. PMLR, 2017.
- [18] H Brendan McMahan, Daniel Ramage, Kunal Talwar, and Li Zhang. Learning differentially private recurrent language models. *arXiv preprint arXiv:1710.06963*, 2017.
- [19] Ilya Mironov. Rényi differential privacy. In *2017 IEEE 30th computer security foundations symposium (CSF)*, pages 263–275. IEEE, 2017.
- [20] Razvan Pascanu and Yoshua Bengio. Revisiting natural gradient for deep networks. *arXiv preprint arXiv:1301.3584*, 2013.

- [21] Sashank Reddi, Zachary Charles, Manzil Zaheer, Zachary Garrett, Keith Rush, Jakub Konečný, Sanjiv Kumar, and H Brendan McMahan. Adaptive federated optimization. *arXiv preprint arXiv:2003.00295*, 2020.
- [22] Mrinmay Sen, A Kai Qin, Yen-Wei Chen, Balasubramanian Raman, et al. Sofim: Stochastic optimization using regularized fisher information matrix. In *2024 International Joint Conference on Neural Networks (IJCNN)*, pages 1–7. IEEE, 2024.
- [23] Jack Sherman and Winifred J Morrison. Adjustment of an inverse matrix corresponding to a change in one element of a given matrix. *The Annals of Mathematical Statistics*, 21(1):124–127, 1950.
- [24] Yuqing Zhu, Jinshuo Dong, and Yu-Xiang Wang. Optimal accounting of differential privacy via characteristic function. In *International Conference on Artificial Intelligence and Statistics*, pages 4782–4817. PMLR, 2022.

A Hockey-Stick Divergence and Privacy Accounting

We present the exact privacy accounting method used to calibrate the noise multiplier σ_g for a target privacy budget (ϵ, δ) over T federated rounds under full client participation.

Our implementation follows the record-level DP-FedGD mechanism (Algorithm 5), where each client adds Gaussian noise to the sum of clipped per-example gradients before normalization, and the server aggregates all client updates. Privacy is accounted for using the exact Hockey-Stick (HS) divergence for the Gaussian mechanism.

A.1 Privacy Mechanism Parameters

The privacy mechanism is defined by the following parameters:

- Clipping threshold: C_g (per-example gradient norm bound)
- Noise multiplier: σ_g
- Number of clients: n (full participation every round)
- Local dataset size: $|\mathcal{D}_i|$ for client i
- Number of rounds: T

At round t , each client releases

$$u_i^t = \frac{1}{|\mathcal{D}_i|} \left(\sum_{(x,y) \in \mathcal{D}_i} \text{clip}_{C_g}(\nabla f(\theta^t; x, y)) + E_i^t \right), \quad E_i^t \sim \mathcal{N}\left(0, \frac{(C_g \sigma_g)^2}{n} I_d\right), \quad (56)$$

and the server forms the aggregated update

$$U^t = \frac{1}{n} \sum_{i=1}^n u_i^t. \quad (57)$$

A.2 Record-Level Sensitivity

We adopt record-level replace-one adjacency: two federated datasets are neighboring if they differ by one record in one client's local dataset.

For client i , changing one record can change the clipped gradient sum by at most $2C_g$. After normalization by $|\mathcal{D}_i|$, the ℓ_2 sensitivity of the released update is:

$$\Delta_i = \frac{2C_g}{|\mathcal{D}_i|}. \quad (58)$$

For a conservative global guarantee, we upper bound using the minimum dataset size $|\mathcal{D}_{\min}| = \min_i |\mathcal{D}_i|$, yielding:

$$\Delta = \frac{2C_g}{|\mathcal{D}_{\min}|}. \quad (59)$$

A.3 Noise Scale of Released Updates

Each client adds noise $E_i^t \sim \mathcal{N}(0, \frac{(C_g \sigma_g)^2}{n} I_d)$ to the sum of clipped gradients and then divides by $|\mathcal{D}_i|$. Therefore, the noise standard deviation of the released client update u_i^t is:

$$\sigma_{\text{release}} = \frac{C_g \sigma_g}{\sqrt{n} |\mathcal{D}_i|}. \quad (60)$$

In privacy accounting, we conservatively use $|\mathcal{D}_{\min}|$ in place of $|\mathcal{D}_i|$.

We account for privacy of the per-client released updates $\{u_i^t\}_{t=1}^T$ observed by the server. The factor $1/\sqrt{n}$ arises from the Algorithm-5 noise parameterization and should not be interpreted as subsampling amplification.

A.4 Hockey-Stick Divergence Composition

For a single application of the Gaussian mechanism with sensitivity Δ and noise standard deviation σ_{release} , the exact privacy loss under the Hockey-Stick divergence is given by:

$$\delta(\epsilon) = \Phi\left(-\frac{\epsilon\sigma_{\text{release}}}{\Delta} + \frac{\Delta}{2\sigma_{\text{release}}}\right) - e^\epsilon \Phi\left(-\frac{\epsilon\sigma_{\text{release}}}{\Delta} - \frac{\Delta}{2\sigma_{\text{release}}}\right), \quad (61)$$

where Φ is the standard normal cumulative distribution function.

For T rounds with independent noise draws, the composed privacy guarantee is:

$$\delta(\epsilon) = \Phi\left(-\frac{\epsilon\sigma_{\text{release}}}{\sqrt{T}\Delta} + \frac{\sqrt{T}\Delta}{2\sigma_{\text{release}}}\right) - e^\epsilon \Phi\left(-\frac{\epsilon\sigma_{\text{release}}}{\sqrt{T}\Delta} - \frac{\sqrt{T}\Delta}{2\sigma_{\text{release}}}\right). \quad (62)$$

A.5 Substituting Mechanism Parameters

Substituting

$$\Delta = \frac{2C_g}{|\mathcal{D}_{\min}|}, \quad \sigma_{\text{release}} = \frac{C_g\sigma_g}{\sqrt{n}|\mathcal{D}_{\min}|},$$

we obtain

$$\delta(\epsilon) = \Phi\left(\frac{\sqrt{nT}}{\sigma_g} - \frac{\epsilon\sigma_g}{2\sqrt{nT}}\right) - e^\epsilon \Phi\left(-\frac{\sqrt{nT}}{\sigma_g} - \frac{\epsilon\sigma_g}{2\sqrt{nT}}\right). \quad (63)$$

A.6 Numerical Calibration

Given target (ϵ, δ) , we solve for σ_g via binary search over a predefined range (e.g., $[0.01, 5000]$) to find the smallest value satisfying:

$$\delta(\epsilon) \leq \delta. \quad (64)$$

This procedure is repeated until convergence within a specified tolerance. This is the exact procedure implemented in our Hockey-Stick accountant.

A.7 Full Participation (No Subsampling Amplification)

Our implementation uses full client participation in every round ($K = n$), and therefore there is **no subsampling amplification**. The privacy accounting above directly applies without any amplification factor.

A.8 Why Hockey-Stick vs. RDP?

The Hockey-Stick divergence computes the exact privacy loss distribution for the Gaussian mechanism, yielding the tightest possible (ϵ, δ) guarantees. In contrast, Rényi differential privacy (RDP) provides only an upper bound via moment-based analysis. In practice, HS/Gaussian-DP accounting can be tighter than RDP-based bounds for the same target (ϵ, δ) , allowing smaller noise multipliers and improved utility.

A.9 Post-Processing and SOFIM Preconditioning

The SOFIM preconditioning step operates only on the privatized aggregated updates $\{U^t\}$ and does not access the raw client data.

By the post-processing theorem of differential privacy [9], any data-independent transformation applied to the output of a differentially private mechanism preserves the privacy guarantee. Since momentum accumulation, Fisher proxy construction, and the Sherman–Morrison inversion are deterministic functions of $\{U^t\}$, they incur no additional privacy cost. Therefore, DP-FedSOFIM satisfies (ϵ, δ) -DP with privacy parameters determined solely by the DP-FedGD mechanism and its composition over T rounds.